Experiments on the Self-Organized Critical State of ^{4}He

A. R. Chatto[1], R. A. M. Lee[2], R. V. Duncan[3], and D. L. Goodstein[2]

[1] *Department of Physics, Brown University, Providence, RI 02912, USA*
[2] *Condensed Matter Physics, California Institute of Technology, Pasadena, CA 91125, USA*
[3] *Department of Phsics and Astronomy, University of New Mexico, Albuquerque, NM 87131-1156, USA*

*When a heat flux Q is applied downward through a sample of ^{4}He near the lambda transition, the helium self organizes such that the gradient in temperature matches the gravity-induced gradient in T_λ. All the helium in the sample is then at the same reduced temperature $t = \frac{T-T_\lambda}{T_\lambda}$ and the helium is said to be in the Self-Organized Critical (SOC) state. We have made the first measurements of the ^{4}He SOC state specific heat, $C_{\nabla T}(T(Q))$. There is no measurable difference between $C_{\nabla T}$ and the static zero-gravity ^{4}He specific heat for temperatures between 250 and 650 nK below T_λ. Closer to T_λ, the specific heat is depressed and reaches a maximum value at 50 nK below T_λ. This depression is similar to that predicted theoretically [R. Haussmann, Phys. Rev. B, **60**, 12349 (1999)]. Contrary to the expectations of theory, however, we see another depression far below T_λ. In addition, over the heat flux range of 30 nW/cm^2 to 13 μW/cm^2, we have made improved measurements of the speed of a recently discovered propagating thermal mode, which travels only upstream against the nominal heat flux of the SOC state. We are able to accurately compute the speed of this wave by treating the helium of SOC state as a traditional fluid with a temperature dependent thermal conductivity.*

PACS numbers: 67.40.Pm, 05.65.+b, 05.70.Jk

1. INTRODUCTION

In the presence of gravity and very close to the superfluid transition temperature T_λ, ^{4}He under a heat flux forms a Self-Organized Critical (SOC) state. The state was predicted to exist on the normal side of the transition[1]. Gravity creates a hydrostatic pressure gradient[2] in the helium which results in a gradient in T_λ of $\nabla T_\lambda = 1.273\ \mu$K/cm. The thermal conductivity κ is a very strong function of temperature and in the low heat flux limit diverges with $\kappa(t) \to \infty$ as $t \to 0$, where t is the reduced temperature $t = \frac{T-T_\lambda}{T_\lambda}$. When a heat flux Q is applied downward through a sample of helium, the resulting temperature gradient parallels the gradient in T_λ, and the helium self organizes to satisfy the condition

$$Q/\kappa = \nabla T_\lambda. \tag{1}$$

The process is self-correcting. If $\kappa(t)$ is too large/(small) at a particular height in the sample, the gradient is smaller/(larger) than ∇T_λ and t grows/(shrinks) with decreasing height and κ converges to the solution to eq. (1). As shown in fig. 2, when the SOC state is achieved, the reduced temperature is uniform even though there is a temperature gradient.

Ten years after its prediction, the SOC state in ^{4}He was observed for the first time by Moeur *et al.*[3] Unexpectedly, they saw not only the normal phase SOC state, but also self-organization at temperatures below T_λ at higher heat flux. They were able to explain their results by positing that κ diverged not at T_λ but at $T_{\mathrm{DAS}}(Q)$, where $T_{\mathrm{DAS}}(Q)$ is the measured temperature at which the perfect thermal conductivity of the superfluid state fails abruptly under a heat flux Q applied upwards through the helium.[4] This encouraged the interpretation that the heat flux was depressing the critical point T_λ to the lower $T_\lambda(Q) = T_{\mathrm{DAS}}(Q)$ and that the SOC state was therefore always on the 'normal' side of T_λ. An alternate explanation of the SOC state below T_λ was later presented by Weichman and Miller.[5] They used a one dimensional theoretical model that treated the high-heat-flux self organization as a superfluid with a series of phase slips. The resulting temperature profile as a function of position resembles a staircase and is shown in fig. 1. These phase slips are dynamic entities which travel upwards through the SOC state.

Weichman and Miller also explored the SOC state above T_λ. They predicted the existence of a thermal wave that would travel only upwards against the flow of the nominal heat flux of the SOC state. This SOC wave was subsequently observed both above *and* below T_λ by Sergatskov *et al.*[6]

In an attempt to probe the nature of the SOC state of ^{4}He, especially as it relates the the critical phase transition at T_λ, we performed two experiments. First, we measured the specific heat of the SOC state. If the critical

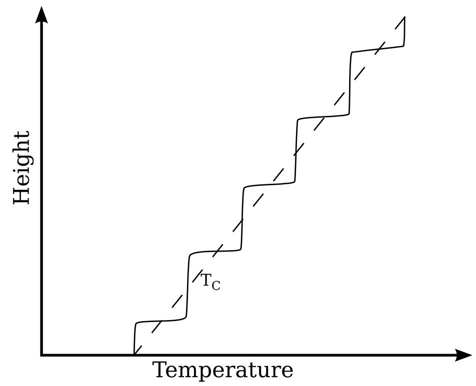

Fig. 1. Schematic of the staircase SOC state profile in the Weichman and Miller model [5].

point temperature T_λ were depressed by the SOC heat flux as suggested by the Moeur *et al.* results, then there should be some significant effect on the specific heat anomaly at T_λ. Second, we did a systematic study of the speed of the SOC wave both above and below T_λ. We hoped to find out if there was some difference in the behavior of this wave on either side of T_λ.

2. The Apparatus

Our cell has two gold-plated copper endplates glued to an insulating Vespel sidewall which gives a cylindrical sample 2.54 cm tall and 2.3 cm in diameter. We have three high resolution thermometers (HRTs); one on each of the top and bottom endplates and a third on a 165 μm thick copper foil that penetrates the sidewall. This foil is positioned one quarter of the way up the sample and is in direct contact with the helium. We measured the size of our helium sample to be 0.389$\pm$0.001 moles through a calibrated extraction.

3. Specific Heat of the SOC State

Measuring the specific heat of the SOC state is unlike traditional heat capacity experiments. The only way to change the temperature of the SOC state is to change the heat flux traveling through it. The procedure involves fully establishing the SOC state at one heat flux, switching to a new heat flux, and then measuring the amount of energy needed to fully establish the

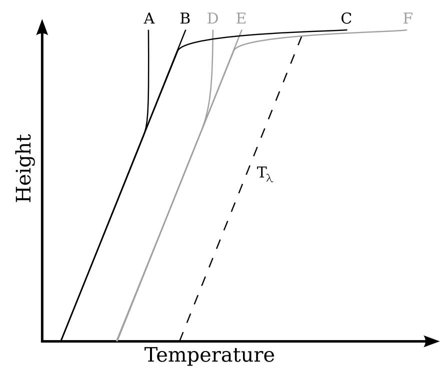

Fig. 2. Profiles of helium temperature vs. sample height during the experimental procedure. The labels are explained in the text.

SOC state at the new heat flux. A schematic of the temperature profiles during the procedure is presented in fig. 2. One set of time series data for the top and midplane thermometers is shown in fig. 3. Each iteration of this procedure produces one heat capacity measurement at one temperature and heat flux.

Initially (time $t = 0$ s and profile **A**), a heat flux Q_1 flows through the SOC state. The self organization extends most of the way through the sample with a small amount of superfluid near the top. A heater on the top endplate of the cell provides the SOC heat flux Q_1 so the sample is in quasistatic equilibrium. At $t = 6$ s, the top heater is increased by δH which causes the superfluid layer to warm and shrink as more of the sample enters the SOC state. Eventually (time $t_1 = 31$ s and profile **B**), the SOC state is fully formed and the derivative of the top HRT reaches a maximum. Normal fluid then penetrates at the top of the cell and results in profile **C**. At $t = 36$ s, the heaters at the top and bottom of the cell are adjusted so that $Q_2 < Q_1$ flows out from the bottom of the sample and the excess heat applied by the top heater is still δH. In less than a second, the sample settles into the new SOC state with an SOC temperature $\Delta T \approx 20$ nK warmer and the superfluid layer reformed at the top of the sample, as shown in profile **D**. The fully formed SOC state at the new heat flux Q_2 (profile **E**) is reached at $t_2 = 52$ s. Normal fluid again penetrates at the top of the cell. Then, the entire procedure is reversed, removing δH throughout and switching back to the original heat flux Q_1.

The heat capacity derived from this procedure is

$$C_{\nabla T} = \frac{\delta H(t_4 - t_3 + t_2 - t_1)}{2\Delta T}. \tag{2}$$

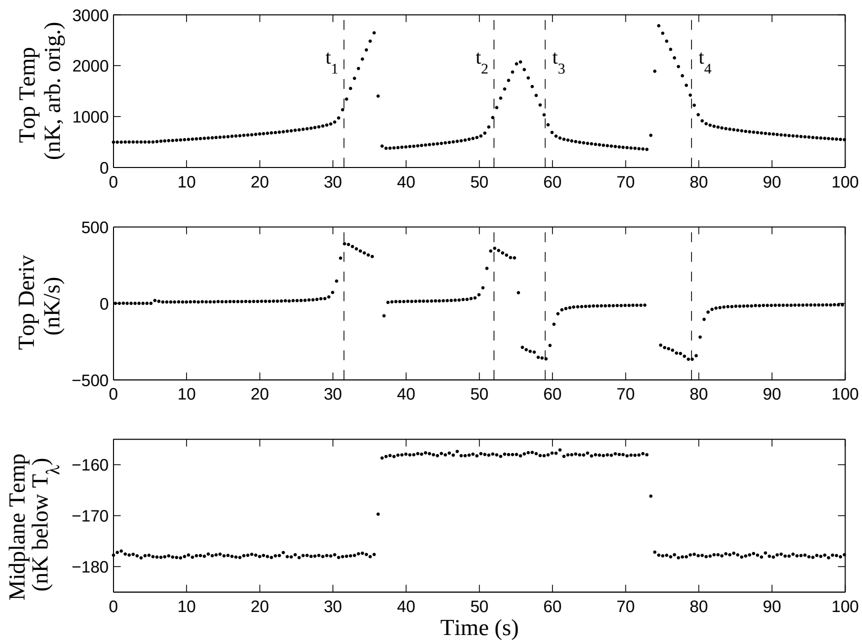

Fig. 3. Data time series for one SOC heat capacity data point. The initial heat flux is $Q_1 = 1.47\,\mu\mathrm{W/cm}^2$ and the second is $Q_2 = 1.27\,\mu\mathrm{W/cm}^2$.

The results from our measurements are presented in fig. 4. In addition, we have plotted the static zero-gravity specific heat and two Dynamic Renormalization Group (DRG) predictions for $C_{\nabla T}$ from R. Haussmann[7]. Over the range of 650 to 250 nK below T_λ, the experimental results agree with the static heat capacity. Closer to T_λ, the specific heat is depressed compared to the static case and reaches a maximum at 50 nK below T_λ. This peak is evidence of the superfluid phase transition and evidence against the notion of a depressed $T_\lambda(Q)$. A mechanism similar to that proposed by Weichman and Miller is necessary to explain the SOC temperature gradient. In the static case, the near divergence of the specific heat is caused by an increase in the size and frequency of fluctuations between the two phases, normal and superfluid, near the critical phase transition. A staircase temperature profile would limit the maximum size of these fluctuations and could lead to the observed depression in the specific heat very close to T_λ.

The depression near T_λ is similar to the predictions of Haussmann. His second prediction, which includes a reasonable estimation of the energy contribution of the vortex cores, is within 1% of the experimental data. However, the experimental data also shows a large unpredicted depression at temperatures below 650 nK below T_λ.

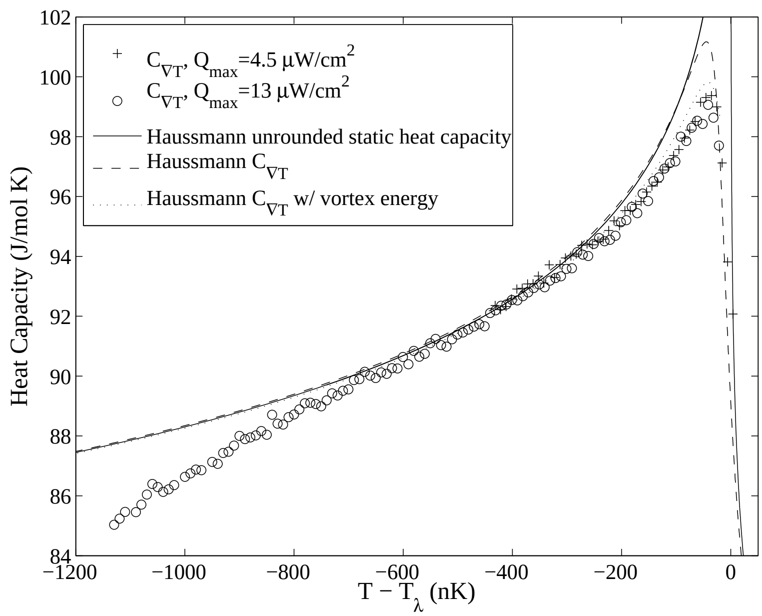

Fig. 4. Specific heat of the SOC state results. The different symbols represent data runs with different maximum heat flux.

4. The SOC Wave

In order to model the SOC wave, we start with the regular heat transfer equations, $C\frac{\partial T}{\partial t} = -\vec{\nabla} \cdot \vec{Q}$ and $\vec{Q} = -\kappa\vec{\nabla}T$. Combining the equations and restricting ourselves to the one dimension of interest, we get

$$C\frac{\partial T}{\partial t} = \frac{\partial}{\partial z}\left(\kappa\frac{\partial T}{\partial Z}\right). \tag{3}$$

This situation is different from regular diffusive heat flow because κ is a strong function of temperature. What results is a temperature/conductivity wave. We transform T to a reduced temperature $\epsilon = (T - T_\lambda)/T_\lambda$, treat the thermal conductivity as a function of ϵ and $\epsilon' = \frac{\partial \epsilon}{\partial z}$ and drop small terms to get

$$CT_\lambda\frac{\partial \epsilon}{\partial t} = \frac{dT_\lambda}{dz}\frac{\partial \kappa}{\partial \epsilon}\frac{\partial \epsilon}{\partial z} + \left(\frac{dT_\lambda}{dz}\frac{\partial \kappa}{\partial \epsilon'} + \kappa T_\lambda\right)\frac{\partial^2 \epsilon}{\partial z^2}. \tag{4}$$

Putting in a trial wave solution of $\epsilon(z,t) = \epsilon_0 + \delta_0 e^{-Dk^2t}e^{ik(z-vt)}$ and solving for the velocity gives

$$v = -\frac{1}{CT_\lambda}\frac{dT_\lambda}{dz}\frac{\partial \kappa}{\partial \epsilon}. \tag{5}$$

Notice that the wave travels only in one direction, upwards against the nominal heat flux of the SOC state. The dissipation D is given by

$$D = \frac{\kappa}{C} + \frac{1}{CT_\lambda}\frac{dT_\lambda}{dz}\frac{\partial\kappa}{\partial\epsilon'}. \tag{6}$$

These can be simplified by realizing that the nominal heat flux of the SOC state is related to the thermal conductivity by $Q_{\mathrm{SOC}} = \kappa\frac{dT_\lambda}{dz}$. This leads to the simple equations

$$v = -\frac{1}{C}\frac{\partial Q_{\mathrm{SOC}}}{\partial T} \tag{7}$$

$$D = \frac{1}{C}\frac{\partial Q_{\mathrm{SOC}}}{\partial T'}. \tag{8}$$

The velocity, therefore, can easily be extracted from a plot of T_{SOC} vs. Q. For the dissipation, however, one needs to know how the heat flux is related to the gradient in temperature, to which we do not have access.

We measured the velocity of the SOC wave by using the phase accumulation technique developed elsewhere[6]. In this technique, a small sinusoidal heat is applied to the bottom heater of a sample of superfluid helium with a downwards heat flux. The sample is allowed to slowly warm and the SOC state starts to form at the bottom of the cell. The time delay for the signal to travel through the helium sample grows with the size of the SOC layer and the velocity can be extracted from the slope of the time delay versus the height of the SOC layer.

The results of our velocity measurements are given in fig. 5. The prediction is from eq. 7, where $C_{\nabla T}$ and $\frac{\partial Q_{\mathrm{SOC}}}{\partial T}$ come from our current measurements. The theoretical curve has treated the SOC state over the entire range of temperatures as a normal fluid phenomenon, albeit with a strongly temperature dependent thermal conductivity.

5. Conclusion

Our two sets of results seem to yield contradictory conclusions. The specific heat results suggest that the superfluid phase transition has occurred as in the static case. However, in our treatment of the velocity of the SOC wave, we treated the SOC state as a normal fluid over the entire temperature range with great success. This begs the question: is the SOC state below T_λ superfluid or normal fluid helium? The staircase temperature profile of Weichman and Miller gives a possible answer: the answer depends on the length scale in question. For the specific heat results, a sample with a staircase profile will appear as a superfluid if the distance between staircase

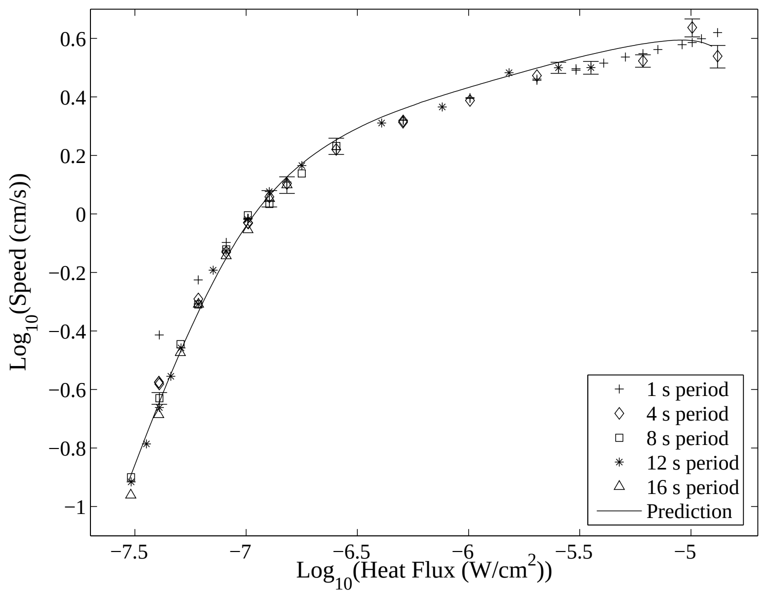

Fig. 5. Wave speed vs. heat flux compared to the prediction of eq. (7). As discussed in the text, this prediction has no adjustable parameters; the values for both the heat capacity and T_{SOC} vs. Q are from our experimental data.

steps is much larger than the maximum size of correlated fluctuations ξ. At 50 nK below T_λ, $\xi \approx 0.005$ cm. For the SOC wave results, if the wave length is much larger than the size of a step, the wave will see the average thermal conductivity of many steps. In our case, the smallest wavelength is 0.4 cm. In this manner, the sample can have a normal fluid thermal conductivity and a superfluid specific heat.

ACKNOWLEDGMENTS

We would like to thank Dmitri Sergatskov, Steve Boyd, Alex Babkin, Alexander Churilov, and Talso Chui for helpful discussions and assistance with cell construction and cryovalve assembly and operation. This work was supported in part by the Fundamental Physics Discipline of the Microgravity Science Office of NASA.

REFERENCES

1. A. Onuki, *Jpns. J. Appl. Phys.*, **26-S3**, 365 (1987).
2. G. Ahlers, *Phys. Rev. Lett.*, **171**, 275 (1968).
3. W. A. Moeur, P. K. Day, F-C. Liu, S. T. P. Boyd, M. J. Adrianns, and R. V. Duncan, *Phys. Rev. Lett.*, **78**, 2421 (1997).
4. R. V. Duncan, G. Ahlers, and V. Steinberg, *Phys. Rev. Lett.*, **60**, 1522 (1988).
5. P. B. Weichman, and J. Miller, *J. Low Temp. Phys.*, **119**, 155 (2000).
6. D. A. Sergatskov, A. V. Babkin, S. T. P. Boyd, R. A. M. Lee,and R. V. Duncan, *J. Low Temp. Phys.*, **134**, 517, (2004).
7. R. Haussmann, *Phys. Rev. B*, **60**, 12349 (1999).